FISEVIER

Contents lists available at ScienceDirect

#### Materials Research Bulletin

journal homepage: www.elsevier.com/locate/matresbu



## Novel hole selective CrO<sub>x</sub> contact for dopant-free back contact silicon solar cells



Wenjie Lin<sup>a,b</sup>, Weiliang Wu<sup>b</sup>, Jie Bao<sup>b</sup>, Zongtao Liu<sup>c</sup>, Kaifu Qiu<sup>a</sup>, Lun Cai<sup>a,b</sup>, Zhirong Yao<sup>a,b</sup>, Youjun Deng<sup>a,b</sup>, Zongcun Liang<sup>a,b,c,\*</sup>, Hui Shen<sup>a,b,c,\*</sup>

- a School of Physics, Sun Yat-Sen University, No. 135 West Xingang Road, Guangzhou, Guangdong Province, 510275, PR China
- b Institute for Solar Energy Systems, School of Physics and State Key Laboratory of Optoelectronic Materials and Technologies, Sun Yat-Sen University, Guangzhou, Guangdong Province, PR China
- <sup>c</sup> Shunde-SYSU Institute for Solar Energy, Beijiao, Shunde, Guangdong Province, 528300, PR China

#### ARTICLE INFO

# Keywords: Chromium trioxide Hole selective contact Dopant-free Back contact Silicon heterojunction solar cells

#### ABSTRACT

The dopant-free back contact solar cells are demonstrated based on hole selective contact material, chromium trioxide ( $CrO_x$ , x < 3) with a low melting point for high stability and high performance. In this contribution,  $CrO_x$  is first applied in silicon based solar cell as the emitter. Integrating 5 nm  $CrO_x$  and 2 nm  $LiF_x$  into solar cell as the emitter and the back surface filed, resulted in a device efficiency of 13.6%. For further improvement, the back contact solar cell reaching an efficiency of 15.8% was fabricated, by implementing the multilayer films of  $CrO_x$  (5 nm)/Au (4 nm)/  $CrO_x$  (5 nm) as the emitter. The formation of  $Cr(OH)_3$  in ambient condition, resulted in a lower work function (4.8 eV) of the  $CrO_x$  film. Furthermore, the multilayer back contact solar cell demonstrated a high stability due to  $CrO_x$  covered with 500 nm Ag, when stored in ambient air longer than 170 days.

#### 1. Introduction

Heterojunction interdigitated back contact (HBC) solar cells have generated considerable interest in silicon photovoltaics with the potential to approach the theoretical power conversion efficiency limit of silicon solar cells of 29.1%. Featuring back contact structures to eliminate metal grid shading at the front surface and intrinsic amorphous silicon (a-Si:H(i)) technology to superiorly passivate the surface of silicon wafer, HBC solar cells have recently achieved a cell efficiency of 26.7% [1]. Nevertheless, further efficiency improvements are confined to relying on the doped a-Si:H prepared by inflammable and explosive precursor gases, adding the complexity of the deposition and parasitic optical loss. The increasing dopant concentration induces high interface defect density and decreases an open circuit voltage ( $V_{\rm OC}$ ).

Transition metal oxides (TMOs) have a wide range of work function values ( $\phi\sim3\text{--}7\,\text{eV}$ ) and a large band gap ( $E_{gap}>3\,\text{eV}$ ) [2], such as MoO<sub>3</sub> [3–7], WO<sub>3</sub> [8,9], V<sub>2</sub>O<sub>5</sub> [10–14], NiO [15], CuO [16,17], TiO<sub>2</sub> [18–20], and HfO<sub>2</sub> [21], making them potential candidates for application in TMO/c-Si heterojunction solar cells, as dopant-free, hole or electron selective contact materials and passivation layer materials [22]. An n-Si solar cell with MoO<sub>3</sub>/a-Si:H as hole selective contact has achieved a V<sub>OC</sub> of 725 mV and a power conversion efficiency of 22.5%, which combines a-Si:H(i)/a-Si:H(n) as electron selective contact [4].

Whereas, a cell efficiency of 19.4% was reported for dopant-free asymmetric heterocontacts solar cells using MoO<sub>3</sub>/a-Si:H and LiF<sub>x</sub>/a-Si:H as hole contact and electron contact [5], respectively. In addition,  $V_2O_5$  and WO<sub>3</sub>/n-Si solar cells have yielded a promising conversion efficiency of 19.7% [12] and 17.9% [8], respectively, among which  $V_2O_5$  on n-Si demonstrated better surface passivation quality and performance than MoO<sub>3</sub> and WO<sub>3</sub> [11,13,14].

However, the results above were achieved by combining a-Si:H(i) as passivation interlayer and a-Si:H(n) or a-SiC<sub>x</sub>:H(n) as the back surface contacts, which made the preparation process more complicated. Additionally, the post-deposition annealing is routinely performed to cure the sputter damage of indium tin oxide; however, this impairs the high work function and carrier selectivity of  $V_2O_5$  and  $MoO_3$ , leading to the degradation of fill factor (FF) and efficiency [8,9]. Moreover,  $V_2O_5$  and  $MoO_3$  remain a concern of air stability, although they have better surface passivation quality and performance than other TMOs on c-Si [11,12,14]. Furthermore, vanadium, molybdenum, and tungsten belong to the rare metal elements [23], and the focus has moved toward exploring other TMOs and various novel structures.

In this study, a novel dopant-free back contact solar cell using substoichiometric chromium trioxide ( $CrO_x$ , x < 3) as the emitter employed in conjunction with n-Si was introduced.  $CrO_x$  has been studied extensively as hole transport material in organic solar cells

<sup>\*</sup> Corresponding authors at: School of Physics, Sun Yat-Sen University, No. 135 West Xingang Road, Guangzhou, Guangdong Province, 510275, PR China. E-mail addresses: liangzc@mail.sysu.edu.cn (Z. Liang), shenhui1956@163.com (H. Shen).

owing to its wide band-gap, high stability, high work function, and good hole-transport properties [24-27]. This makes it a good alternative hole selective contact material for TMO/c-Si heterojunction solar cells. Surprisingly, CrOx has not yet been applied to silicon heterojunction solar cell. Moreover, CrO<sub>3</sub> with a lower melting point of 470 K [27], is more suitable for thermal evaporation deposition, compared with V<sub>2</sub>O<sub>5</sub> and MoO<sub>3</sub>. In this work, we fabricated a novel fully dopantfree back contact solar cell composed of  $CrO_x$  and  $LiF_x$  contacts on the emitter and back surface field (BSF) region separately. The dopant-free back contact solar cell was processed at a temperature of < 40 °C and was based on self-aligned process technology via metal mask patterning technology, which was less expensive and a simpler process of interdigitated back contact solar cells [10]. The composition and the work function of the CrOx film deposited by thermal evaporation were investigated. Furthermore, the influences of CrOx and LiFx thickness on the performance of the dopant-free back contact solar cells were explored. By employing a structure of CrO<sub>x</sub> (5 nm)/Au (4 nm)/CrO<sub>x</sub> (5 nm) as emitter, a multilayer back contact (MLBC) solar cell reaching an efficiency of 15.8%, with a V<sub>OC</sub> of 605.0 mV was demonstrated.

#### 2. Experimental details

#### 2.1. CrOx deposition and characterization

CrO<sub>x</sub> thin film with a thickness of 15 nm were thermally evaporated onto flat n-Si (100) substrates that had resistivity of  $1-3 \Omega \, \text{cm}$  from stoichiometric CrO<sub>3</sub> particle with a deposition rate of 0.2 Å/s in the  $2 \times 10^{-2} \, \text{Pa}$  oxygen partial pressures that were backfilled with oxygen after the chamber reached a base pressure of  $5.0 \times 10^{-4}$  Pa. Raman spectra were determined with a Horiba Jobin Yvon Xplora confocal Raman microscope equipped with a motorized sample stage (Marzhauser Wetzlar, 0.01 mm, 00-24-427-0000). The components were characterized via X-ray photoelectron spectral (XPS) analysis (Thermo ESCALAB 250Xi, Thermo Scientific). To study the valence band region and the work function of CrO<sub>x</sub>, ultraviolet photoelectron spectroscopy (UPS) measurements were performed on a Thermo Scientific Escalab 250Xi using the monochromated He I radiation (21.2 eV) in an ultra-high vacuum chamber with a base pressure of  $2 \times 10^{-7}$  Pa. The UPS spectra were obtained with a sample bias of -5 V in normal emission geometry to obtain secondary electron cutoffs. The cross-section of CrO<sub>x</sub>/Au/CrO<sub>x</sub>/n-Si interfaces were obtained by a focused ion beam lift-out technique and observed with a FEI Tecnai G2 F30 transmission electron microscopy (TEM) operating at 300 kV.

#### 2.2. Cell fabrication and measurements

CrO<sub>x</sub>/n-Si back contact solar cells with an aperture cell area of 4 cm<sup>2</sup> were passivated by 10 nm SiO<sub>2</sub> and 75 nm SiN<sub>x</sub> films, prepared by a plasma enhanced chemical vapor deposition, on one side textured silicon wafer after removal of the native oxide in 10% hydrofluoric acid (see Fig. 1a). Low cost self-aligned processing technology via two metal masks was utilized for the deposition of the emitter and BSF regions in stead of the photolithographic or screen print masking, thus simplifying the fabrication and reducing the production cost of the dopant-free back contact solar cells. The chamber was pumped down to  $5.0 \times 10^{-4}$ Pa and by adjusting the oxygen partial pressure of  $2 \times 10^{-2}$  Pa,  $CrO_x$  $(5, 10, 15 \text{ and } 20 \text{ nm}) \text{ or } CrO_x (5 \text{ nm})/Au (4 \text{ nm})/CrO_x (5 \text{ nm}) \text{ were}$ evaporated onto the emitter at a rate of 0.2 Å/s via the metal mask 1 patterning and covered with an evaporated 500 nm thick Ag electrode. After the mask replaced with the metal mask 2, the LiF<sub>x</sub> (1 and 2 nm)/Al (500 nm) films were evaporated onto the BSF areas with deposition rates of 0.2 and 5.0 Å/s, respectively. The high alignment quality to form a 75 µm gap between the CrO<sub>x</sub>/Ag or CrO<sub>x</sub>/Au/CrO<sub>x</sub>/Ag and the  $\text{LiF}_x/\text{Al}$  illustrates an emitter region of 750  $\mu m$  in half-width, and a BSF region of 260 µm in half-width, reported by our previous work [10]. The finalized dopant-free back contact solar cell is shown in Fig. 1b.

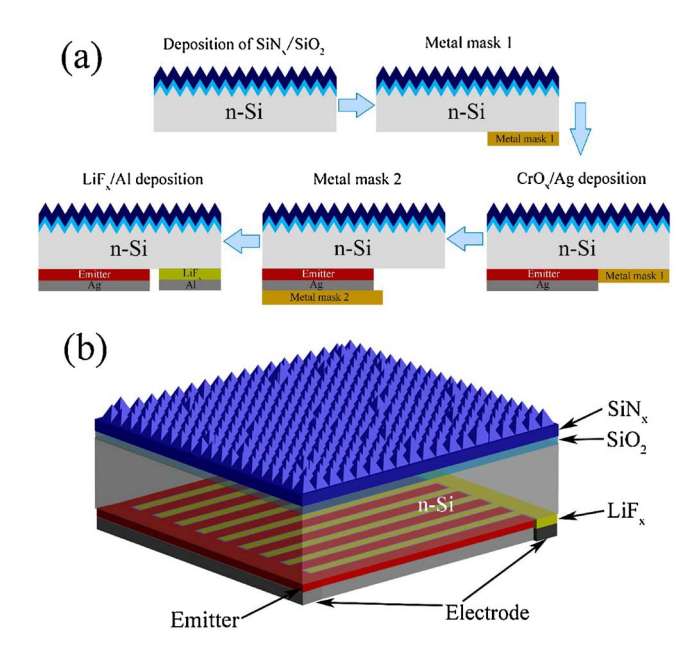


Fig. 1. (a) Schematic of  $CrO_x/n$ -Si back contact solar cell fabrication. (b) The 3D structure of a dopant-free back contact solar cell employing  $CrO_x$  as the emitter.

The light J-V behaviour was measured under standard one sun conditions (100 mW/cm², AM1.5 spectrum, 25 °C) with a  $2\times2$  cm² aperture mask using a solar simulator (Class AAA, Oriel Sol3A, Newport), and the dark J-V behaviour was also investigated. The External Quantum Efficiency (EQE) was conducted using a Solar Cell Quantum Efficiency Measurement System (QEX10, PV Measurements). The  $J_{SC}$  of the solar cell was integrated by the EQE. The injection level dependent open circuit voltage was measured by the transient photoconductance measurement (WCT-120, Sinton).

#### 3. Results and discussion

#### 3.1. The characteristics of CrO<sub>x</sub> film

To correctly interpret the work function of  $CrO_x$  thin film thermally evaporated, it is important to understand their composition. Fig. 2a shows the Raman spectra of  $CrO_x$  thin film,  $CrO_3$  particle (99.99%, Aladdin),  $Cr_2O_3$  powder (99.99%, Aladdin) and n-Si wafer. Owing to the distraction from the Si substrates, the strongest Raman band was ascribed to the Si located at  $521 \ cm^{-1}$ . The characteristic peaks of  $CrO_3$  and  $Cr_2O_3$  at  $532 \ cm^{-1}$  and  $560 \ cm^{-1}$ , respectively, were covered up. However, two characteristic peaks representing  $CrO_3$  were also detected at  $72 \ and \ 299 \ cm^{-1}$ , and the peaks indicating  $Cr_2O_3$  at the bands of  $72 \ cm^{-1}$ ,  $937 \ cm^{-1}$  and  $983 \ cm^{-1}$  were observed, pointing toward the components of  $CrO_3$  and  $Cr_2O_3$  and the partial crystallization of the  $CrO_x$  film as witnessed by X-ray diffraction (not shown). Note that the weak peaks at  $630 \ cm^{-1}$  and  $823 \ cm^{-1}$  for  $Cr(OH)_3$  were observed [28], which is ascribed to very low content in  $CrO_x$ .

The composition of the  $CrO_x$  film were measured by the XPS spectra shown in Fig. 2b). The core level was split into the  $Cr\ 2p_{1/2}$  and  $2p_{3/2}$  doublet centred at a binding energy of 588.7 eV and 579.5 eV, respectively, with a pair of shoulders at lower binding energy, which implied that  $CrO_x$  films were multi-valence state oxide complexes [24]. The relative contents of the diverse  $CrO_x$  films corresponding to the  $Cr\ 2p_{3/2}$  peak were estimated from the fitted Gaussian-Lorentzian curves. It was found that three forms of chromium oxide phase,  $CrO_3$  ( $\approx$ 579.5  $\pm$  0.2 eV),  $Cr(OH)_3$  ( $\approx$ 577.8  $\pm$  0.2 eV) and  $Cr_2O_3$  ( $\approx$ 576.8  $\pm$  0.2 eV) [24,26,27,29,30], existed in the films. The water dissociation and hydroxylation of  $CrO_x$  film exposed to air resulted in the formation of  $Cr(OH)_3$  [26]. The peaks related to  $CrO_2$  ( $\approx$ 575.4 eV) and free chromium ( $\approx$ 574.3 eV) were not observed [24]. The sample

#### Download English Version:

### https://daneshyari.com/en/article/7904606

Download Persian Version:

https://daneshyari.com/article/7904606

<u>Daneshyari.com</u>